Appendices for: experimental testing of a tensegrity simplex: self-stress implementation and static loading

Jonas FERON[1], Landolf RHODE-BARBARIGOS[2], Pierre LATTEUR[3]

[1] Ph.D. Candidate,
Université catholique de Louvain UCLouvain,
Institute of Mechanics, Materials and Civil Engineering IMMC,
Dept. of Civil and Environmental Engineering GCE,
Place du Levant, 1 (Vinci), bte L5.05.01, 1348-Louvain-la-Neuve, Belgium
jonas.feron@uclouvain.be;
BESIX,
Avenue des communautés, 100, 1200 Brussels, Belgium.
jonas.feron@besix.com

[2] Assistant Professor, University of Miami,
College of Engineering, Dept. of Civil & Architectural Engineering
1251 Memorial Drive, McArthur Engineering Bldg., Coral Gables, FL 33146, United States
landolfrb@miami.edu

[3] Professor, Université catholique de Louvain UCLouvain,
Institute of Mechanics, Materials and Civil Engineering IMMC,
Dept. of Civil and Environmental Engineering GCE,
Place du Levant, 1 (Vinci), bte L5.05.01, 1348-Louvain-la-Neuve, Belgium
pierre.latteur@uclouvain.be

NOTATION LIST

The following symbols are used in the appendices:

A_c	[mm²]	Cross-sectionnal area of the cables (horizontal and vertical).
A_i	[mm²]	Cross-sectionnal area of the element (strut or cable) i.
A_s	[mm²]	Cross-sectionnal area of the struts.
$E_{alu,s}$	[MPa]	Measured Young's modulus of the aluminum tubes of the struts.
$E_{alu,c}$	[MPa]	Measured Young's modulus of the aluminum rods of the cables
E_i	[MPa]	Equivalent Young's modulus of the element i (that considers all parts composing the element).
E_{CH}	[MPa]	Equivalent Young's modulus for the horizontal cables (that considers all parts composing the element).
E_{CV}	[MPa]	Equivalent Young's modulus for the vertical cables (that considers all parts composing the element).
E_s	[MPa]	Equivalent Young's modulus for the struts (that considers all parts composing the element).
H_3, H_4, H_5	[mm]	Height of the top nodes of the simplex. Index i (=3, 4, or 5) in H_i relates to the index of the top node. H is used when $H_3 = H_4 = H_5$.
l_i	[mm]	Free length of the element i. Free lengths can be altered by imposed elongations $\{\bar{e}\}$.
$\{t\}$	[N]	Vector of axial forces (tension positive) in the elements.
α_3, α_4, α_5	[°]	Angles of rotation between the top and bottom triangular bases of the simplex. Index i (=3, 4, or 5) in α_i relates to the index of the top nodes. α is used when $\alpha_3 = \alpha_4 = \alpha_5$.

APPENDIX

Appendix A. Form-finding of the tensegrity simplex

Dynamic relaxation [1] was used for the theoretical (i.e. without self-weight) form-finding of the simplex starting from a straight prism configuration i.e. with an angle $\alpha = 0°$ between the horizontal bases and a height H=2043.4mm (Figure 11.a). The struts S1 to S3 are then lengthen by 109.7mm (Figure 11.b) with the resulting equilibrium configuration shown in Figure 11.c. with an angle $\alpha = 30°$ and a height H=1950.0mm. Note that all the intermediate configurations between $\alpha = 0°$ and $\alpha < 30°$ do not possess a self-stress mode and are only stable if all elements are struts. Even when the structure is only made of struts, the configuration $\alpha = 30°$ is only stable if the self-stress level is strictly higher than 0 kN. Therefore, the self-stress state shown in Figure 11.c. is considered as the "zero" self-stress state without self-weight. From this point, elements CB1 to CV3 can be cables. Any further lengthening of the struts S1 to S3 is described in Figure 8 from the self-stress level $a > 0$ kN to $a = 1.5$ kN and in Figure 5.f. from the self-stress level $a = 1.5$ kN to $a_{gov} = 8.81$ kN.

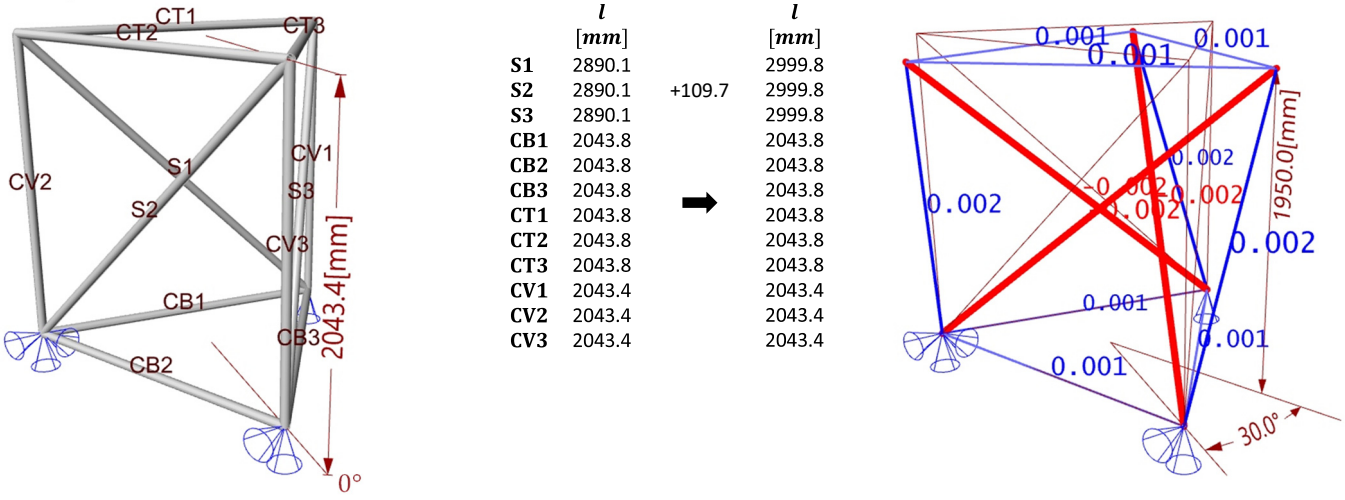

a b c

Figure 11. Simplex form finding without self-weight, a: initial prismatic configuration with $\alpha = 0°$, b: lengthening of the struts, c: resulting equilibrium configuration with $\alpha = 30°$ and the zero self-stress state (in kN).

Appendix B. Prestress implementation and static loading

The actuation principle of the struts and cables is shown in Figure 12. The fine pitch of the M16 threaded rod is 1.5mm per full rotation. The pitch of the M8 turnbuckles is 2*1.25mm per full rotation of the sleeve. To ensure precision, a digital caliper was used to measure variations in reference lengths. The display precision of the digital caliper was +- 0.01mm, with the in-practice precision estimated at +- 0.03mm.

Reference lengths are assumed to be constant, i.e. prestress scenarios that require activating multiple elements are implemented by activating the elements in series while the elastic strains of the reference lengths (due to the prestress forces) are assumed negligible. This assumption seems valid considering that the reference lengths correspond to the threaded rods and turnbuckles made of stainless steel.

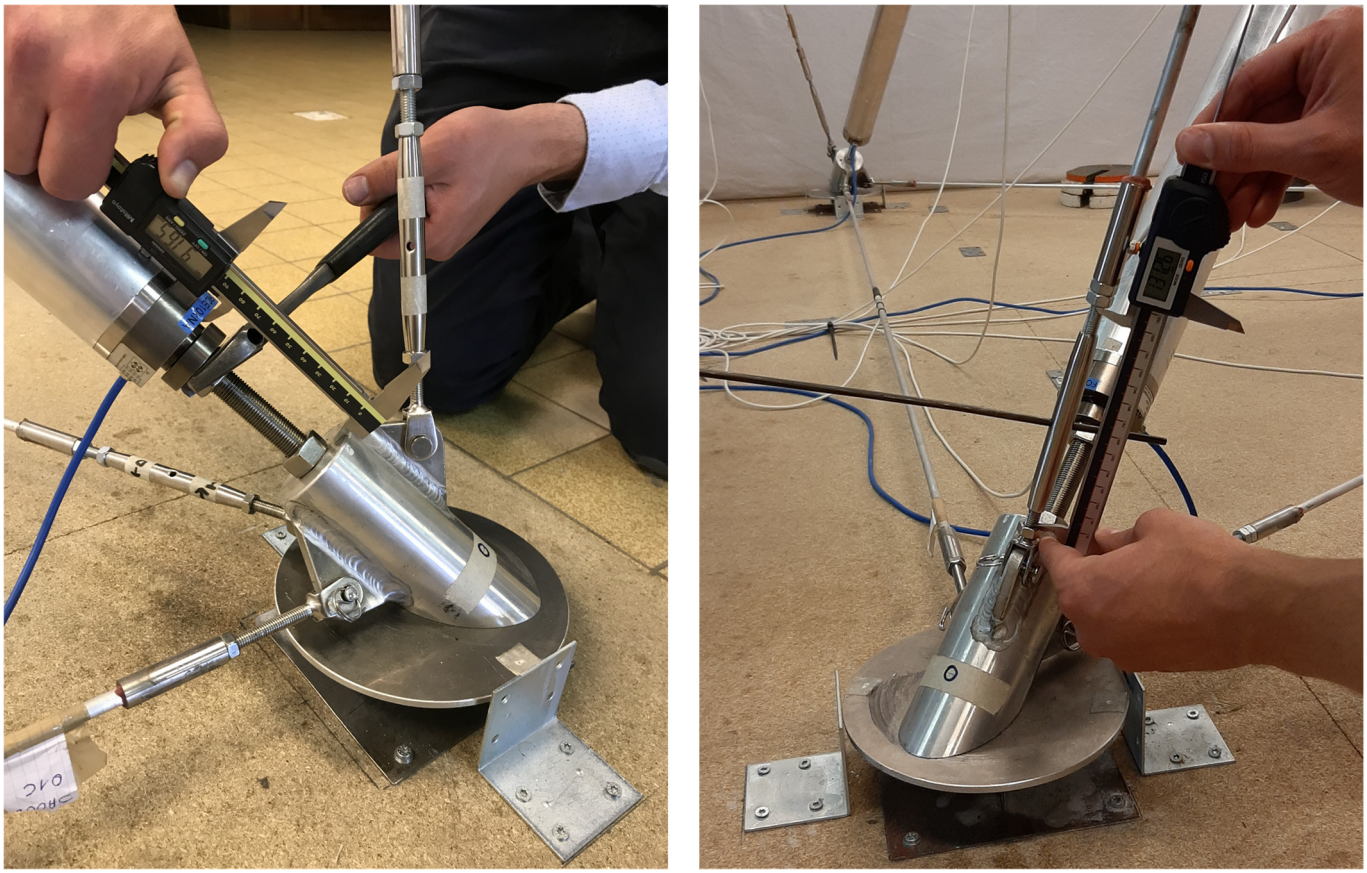

a b

Figure 12. Actuation principle of the reference lengths, a: for strut S3, b: for cable CV3

Figure 13 shows the final pictures for both loading experiments starting from two different self-stress states. Figure 13.a. (resp. b.) corresponds to the final loading stage of Figure 6.a. (resp. b.). In both pictures, the compressive forces in the struts almost reach -10kN but the bending of the struts has more influence in highly distorted geometry i.e. under heavier external loads.

a b

Figure 13. Pictures of loading experiments, a: self-stress level 1.5kN + loading 2.1kN/node, b: self-stress level 8.5kN + loading 0.8kN/node

Appendix C. Mechanical properties of the elements

Table 1 (of main article) shows the Young's moduli E_s, E_{CH}, E_{CV} and cross-sectional areas A_s, A_c, A_c considered in the finite elements model for the three struts, for the six horizontal cables and for the three "vertical" cables respectively. These finite element assumptions are summarized in Figure 14 and are detailed here below. The tubes composing the struts are in aluminum EN-AW6060-ET-T66 [2] but their Young's modulus $E_{alu,s}$=63.40GPa was obtained experimentally in Appendix C.1. Assuming the lower and upper ends of the struts have an infinite stiffness (Figure 14), the Young's modulus of the struts is obtained by $E_s = E_{alu,s}\cdot 2999.8/2700.0 = 70.39$GPa. Similarly the rods composing the cables are in aluminum EN-AW6060-ER-T66 [2] but their Young's modulus $E_{alu,c}$=67.37GPa was obtained experimentally in Appendix C.2. Assuming both joint attachments have an infinite stiffness as well as the turnbuckles and the passive ends have the same Young's modulus $E_{alu,c}$ and area A_c than the rods (Figure 14), the Young's modulus of the horizontal cables is obtained by $E_{CH} = E_{alu,c}\cdot 2043.8/1919.0 = 71.75$GPa. Similarly, the Young's modulus of the "vertical" cables is obtained by $E_{CV} = E_{alu,c}\cdot 2043.4/1907.0 = 72.19$GPa. Joint attachments are considered infinitely stiff because the cylinders used in the joints have a 60mm diameter and are made of aluminum EN-AW-6060 [2], while the gussets are 8mm thick and made of aluminum EN-AW-5754 [2]. Eventually, all struts and cables are assumed perfectly straight as justified in Appendix C.3 and Appendix C.4 with linear elastic behavior while neglecting all bending effects. The finite element model is thus a truss model with geometric non-linearity and initial strains. Note also that the concentric gusset-pin-fork assumption (Figure 14) may be responsible for lengths inaccuracies with non-negligible impact on the initial prestress forces.

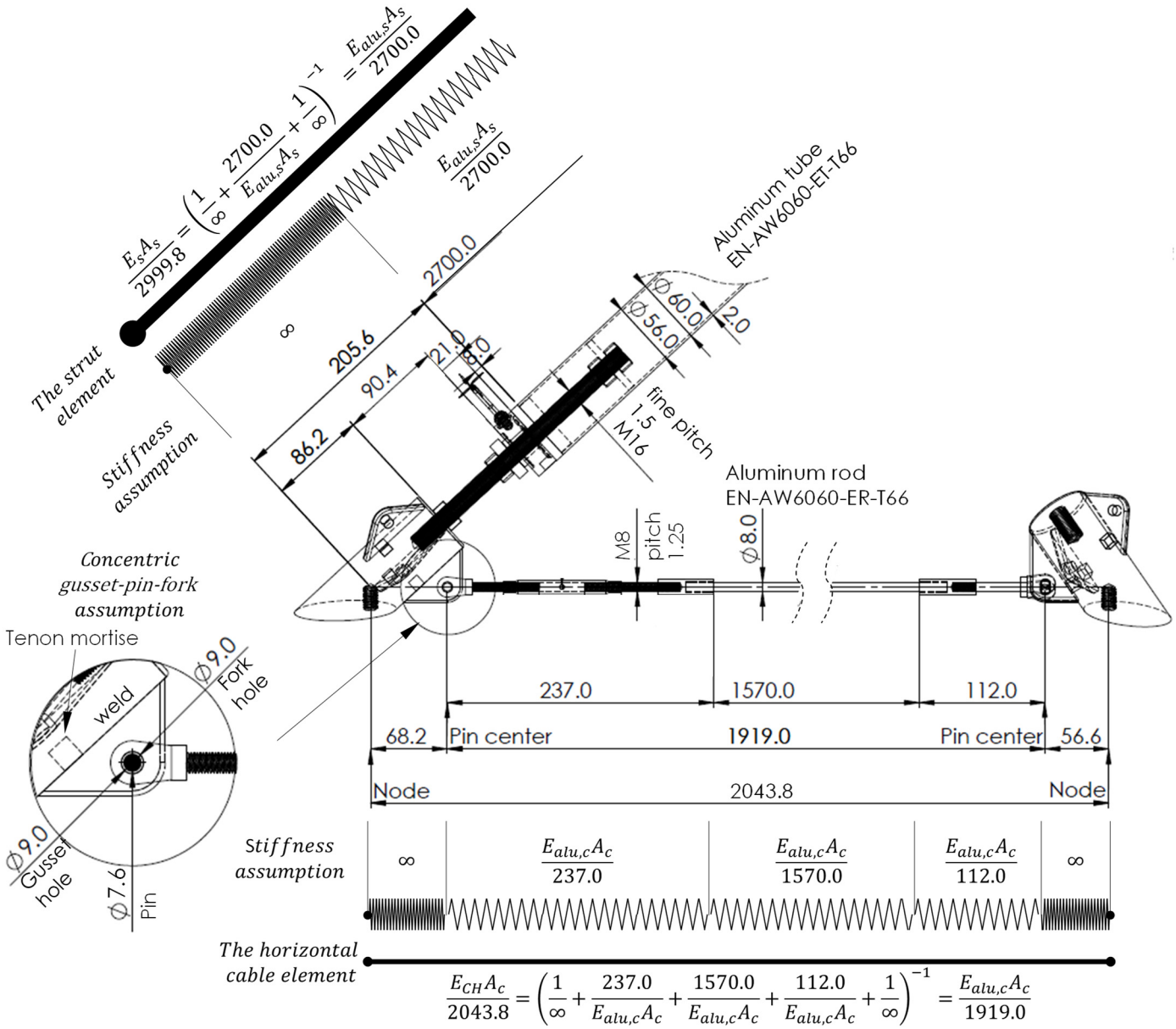

Figure 14. From physical to numerical model: the finite element assumptions

Appendix C.1. Young's modulus $E_{alu,s}$ of aluminum tubes

The Young's modulus $E_{alu,s}$=63.4GPa of the tubes was obtained on the basis of five compression tests (named $Sp1$ to $Sp5$) with a specimen length of 250mm and a specimen slenderness of 12.3 (see [3]). Each specimen was equipped with three strain gauges ($G1$ to $G3$) each distributed 120° around the perimeter. The Young's modulus is calculated based on the averaged strain measured by the three gauges eliminating thus any bending effects. Moreover, the Young's modulus $E_{alu,s}$ of the tubes is taken as the average of the Young's modulus of the five specimens tested computed as the slope of the stress-strain relation between 10kN and 30kN (to disregard the strain hardening of the aluminum).

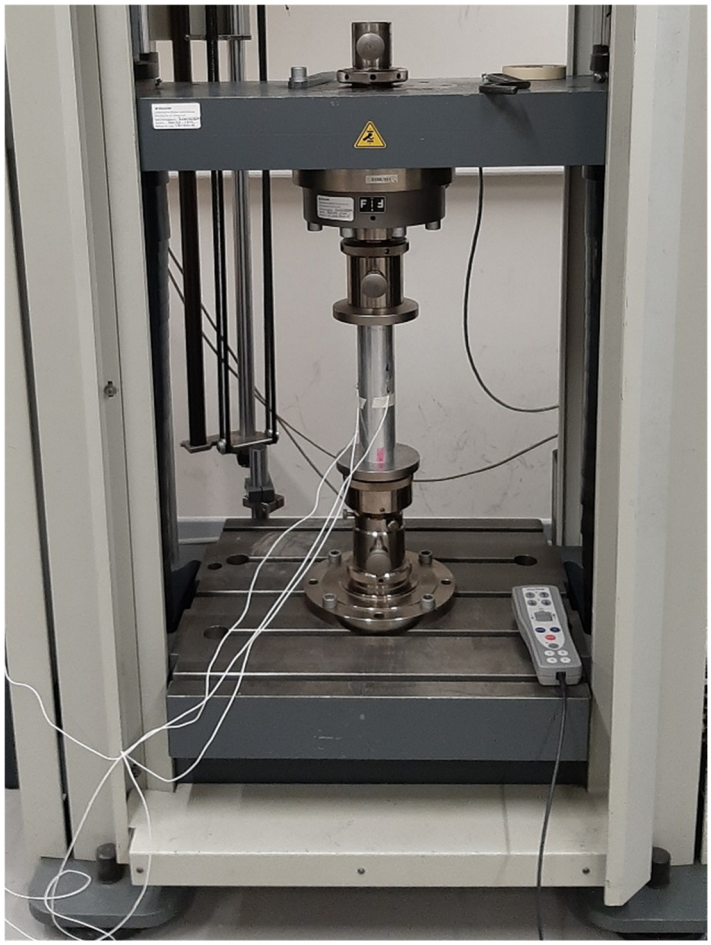

a

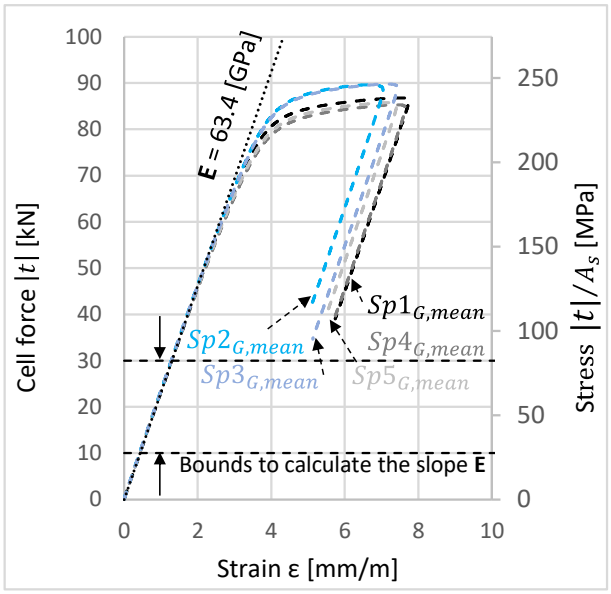

b

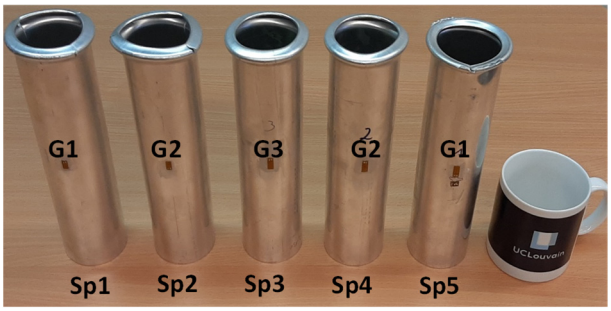

c

Figure 15. Compressive testing on five strut specimens. a: experimental set-up, b) stress-strain relation, c) strut specimens.

Appendix C.2. Young's modulus $E_{alu,c}$ of aluminum rods and strain gauges calibration

To calibrate the strain gauge of each individual cable and to determine the Young's modulus $E_{alu,c}$ of the aluminum rods, three tension tests were performed per cable. Test 1 was disregarded due to the strain hardening of the aluminum. One Young's modulus was defined for each individual cable from the average strain gauge measurements obtained from tests 2 and 3 (Figure 16.b left column). Each individual Young's modulus was used to automatically correlate a measured strain to a measured force in the cable during the prestressing and loading experiments of the simplex. The Young's moduli of the cables E_{CH} and E_{CV} used in the numerical simulations relies on the Young's modulus of the aluminum rods $E_{alu,c}$=67.37GPa measured using an extensometer (Figure 16.c middle column). It is to be noted that, instead of assuming that the turnbuckles have the same stiffness than the aluminum rods, the measurements of the load cell could have been used. The "cell strains" are obtained by dividing the cell displacement by the full length (from pin to pin) of the cables (Figure 16.a). However, the cell displacement includes unknown parasitic displacements of the tension machine MTS100kN itself. Hence the results obtained from the cell displacements are disregarded and are just provided for the record.

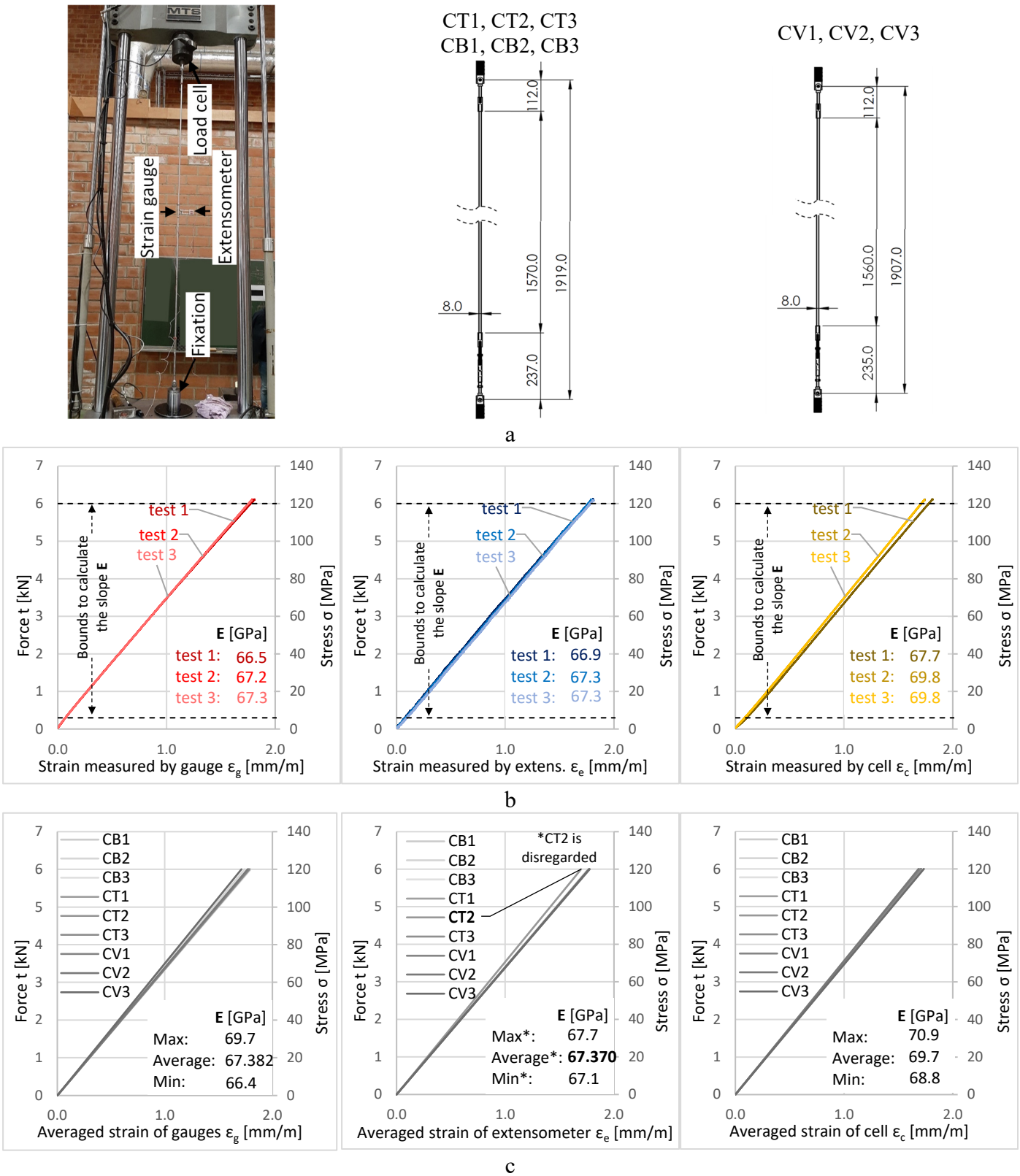

Figure 16. Tensile tests, a: experimental set-up, b: results for the top cable CT3, c: average for all cables and for tests 2 and 3.

Appendix C.3. Straight struts assumption and buckling resistance

A buckling test was performed on a 2999.8mm strut specimen (Figure 17). The strut specimen was not reused in the simplex model. The test allowed concluding that:

- The experimental buckling resistance of the specimen is 14.1kN.
- The relation $t_s - d_z$ is essentially linear until buckling occurs. However a Young's modulus E_s can not be deduced from this test due to the parasitic displacements of the whole testing system.
- The norm of the horizontal displacements $w = \sqrt{d_x^2 + d_y^2}$ at mid-height is assumed negligible up to the buckling resistance of the eurocode. The small w<3mm observed may be due to support condition (M16 into hole of diameter 20mm).

Therefore it is assumed that the struts of the simplex have a bifurcation buckling behavior (Figure 18) and a linear elastic stiffness with Young's modulus E_s=70.39GPa. The considered buckling resistance of the struts is 10.66kN (Eurocode [2]). The Eurocode calculation is further detailed in [3]. It assumes a material EN-AW6060-ET-T66 and a perfect dimension A_s for the entire 2999.8[mm] length as well as perfect hinges at the extremities.

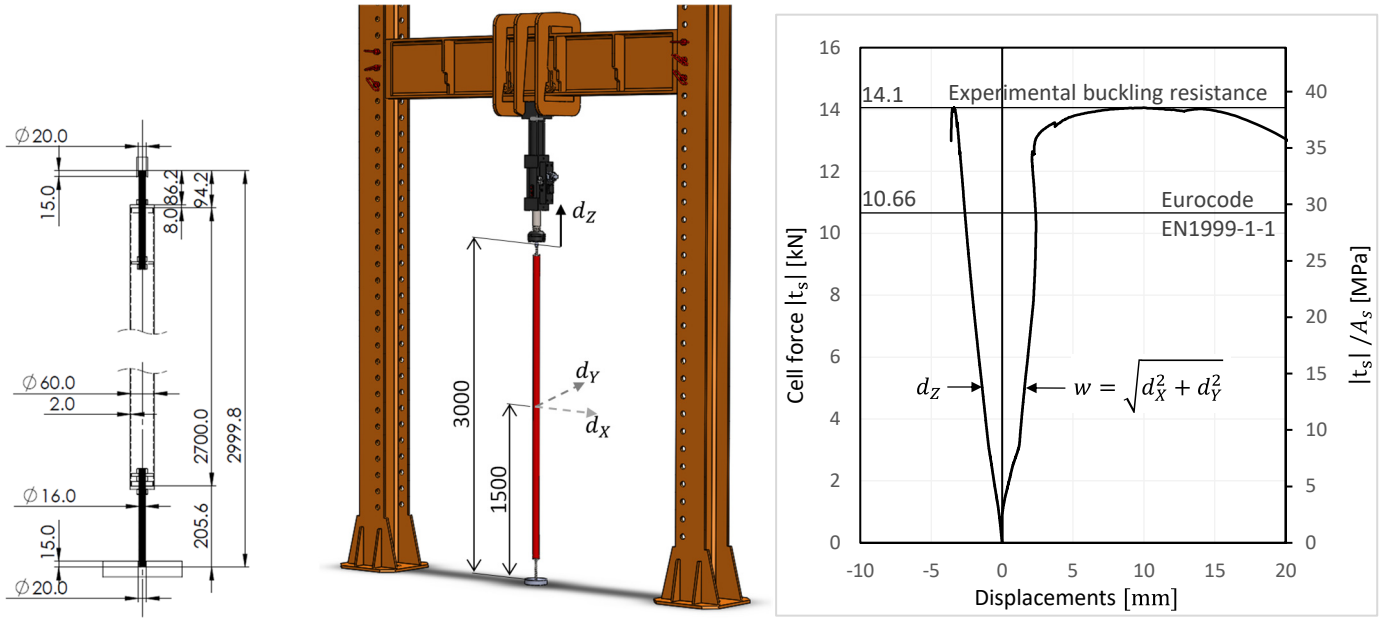

Figure 17. Experimental buckling test, a: dimensions of the tested struts (in [mm]*), b: buckling test set up, c: measured results.*

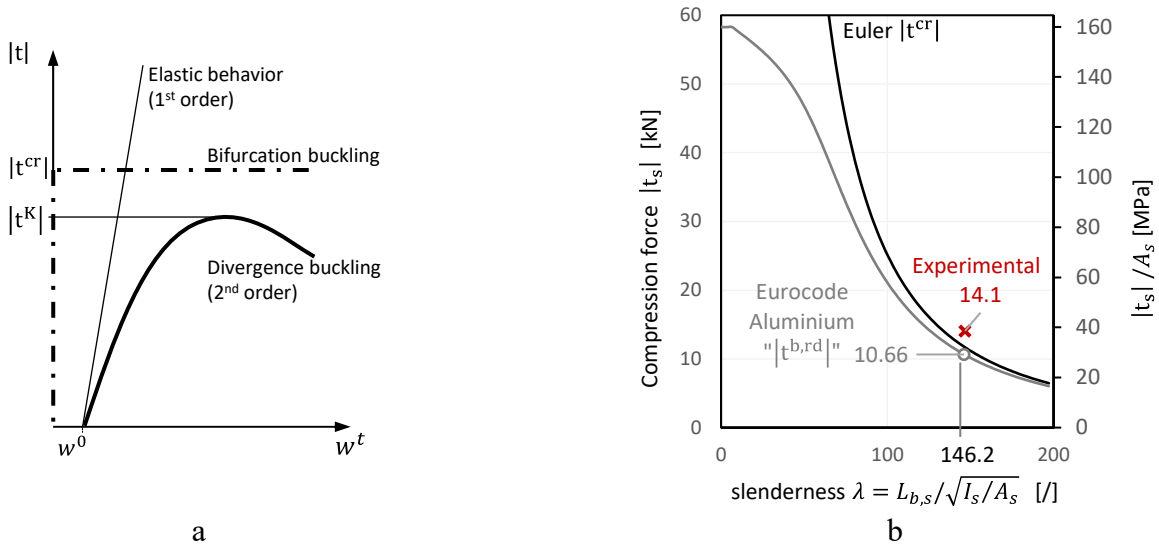

a b

Figure 18. Theorical buckling behavior, a: bifurcation buckling and divergence buckling (adapted and translated from [4]*), b: Eurocode buckling curve* [2].

Appendix C.4. Straight cables assumption

A minimum tension of 0.59kN is required in the horizontal cables to avoid parasitic bending effects due to self-weight (Figure 19). These effects are both a non-linear axial stiffness due to the catenary/bended shape of the cable and a parasitic bending strain in the strain gauge measurements. The minimum tension of 0.59kN was obtained thanks to geometric non-linear calculations using SCIA engineering [5] assuming 1919mm long rod with 8mm diameter in aluminum (of Young's modulus $E_{alu,c}$=67.37GPa and specific mass 2700kg/m³) and with a small bending inertia I_c=201mm^4. When the tension in the horizontal cables is higher than 0.59kN, cables can be assumed perfectly straight (deflection smaller than 1mm) with a linear axial stiffness and parasitic bending strain measured by the strain gauges can be assumed negligible. Note that all strain gauges are reset to 0kN before starting any experiments on the simplex model. Initial tensions in the cables are thus obtained by equilibrium from the measured compressive force in the struts by force sensors.

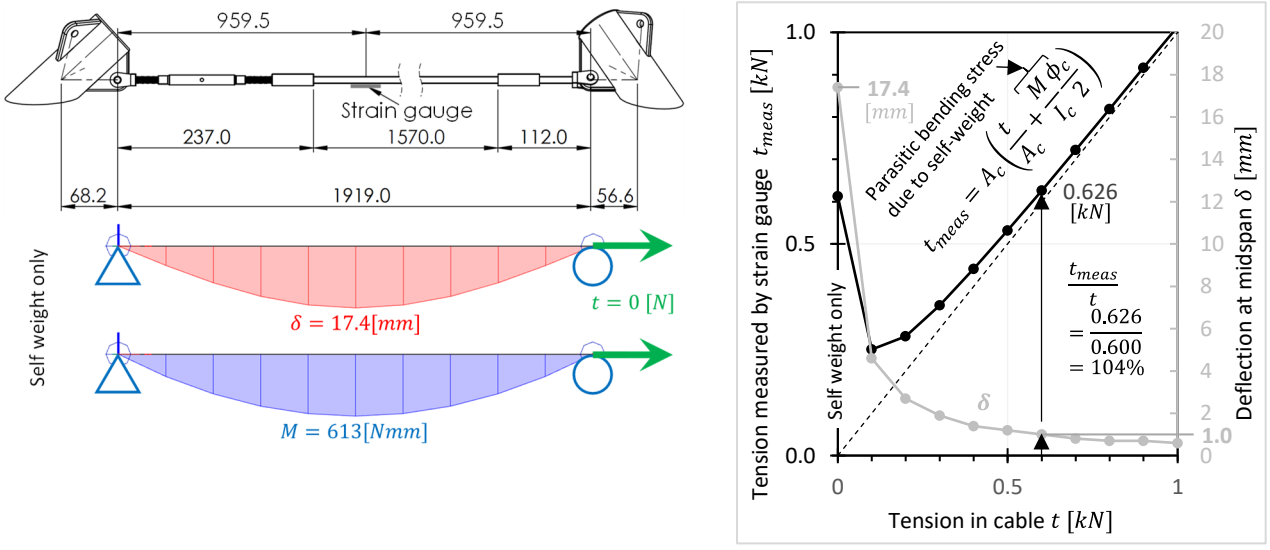

a b

Figure 19. a: Strain gauge attached on the lower side of the rods; b: Parasitic effects due to self-weight before t=0.59 [kN].

REFERENCES

[1] N. Bel Hadj Ali, L. Rhode-Barbarigos, and I. F. C. Smith, "Analysis of clustered tensegrity structures using a modified dynamic relaxation algorithm," *Int. J. Solids Struct.*, vol. 48, no. 5, pp. 637–647, 2011.

[2] CEN, "EN 1999-1-1:2007+A1:2009 - Eurocode 9 - Design of aluminium structures - Part 1-1: General structural rules," 2009.

[3] J. Feron, A. Bertholet, and P. Latteur, "Replication Data for: Experimental testing of a tensegrity simplex: self-stress implementation and static loading," *Open Data @ UCLouvain*, 2022. [Online]. Available: https://doi.org/10.14428/DVN/CDLVFV.

[4] M. A. Hirt, R. Bez, and A. Nussbaumer, *Construction métallique: notions fondamentales et méthodes de dimensionnement*, Volume 10. Traité de Génie Civil de l'EPFL, 2006.

[5] NEMETSCHEK, "SCIA – logiciels de calcul de structure," 2021. [Online]. Available: https://www.scia.net/fr. [Accessed: 13-Dec-2021].